

Resonant inelastic x-ray scattering study of hole-doped manganites $\text{La}_{1-x}\text{Sr}_x\text{MnO}_3$ ($x = 0.2$ and 0.4)

K. Ishii,^{1,*} T. Inami,¹ K. Ohwada,¹ K. Kuzushita,¹ J. Mizuki,¹ Y. Murakami,^{1,2}
S. Ishihara,² Y. Endoh,^{3,4} S. Maekawa,³ K. Hirota,⁵ and Y. Moritomo⁶

¹*Synchrotron Radiation Research Center,*

Japan Atomic Energy Research Institute, Hyogo 679-5148, Japan

²*Department of Physics, Tohoku University, Sendai 980-8578, Japan*

³*Institute for Materials Research, Tohoku University, Sendai 980-8577, Japan*

⁴*International Institute for Advanced Studies,*

Kizugawadai, Kizu, Kyoto 619-0225, Japan

⁵*The Institute for Solid State Physics,*

The University of Tokyo, Chiba 277-8581, Japan

⁶*Department of Applied Physics, Nagoya University, Nagoya 464-8603, Japan*

(Dated: November 16, 2018)

Abstract

Electronic excitations near the Fermi energy in the hole doped manganese oxides ($\text{La}_{1-x}\text{Sr}_x\text{MnO}_3$, $x = 0.2$ and 0.4) have been elucidated by using the resonant inelastic x-ray scattering (RIXS) method. A doping effect in the strongly correlated electron systems has been observed for the first time. The scattering spectra show that a salient peak appears in low energies indicating the persistence of the Mott gap. At the same time, the energy gap is partly filled by doping holes and the energy of the spectral weight shifts toward lower energies. The excitation spectra show little change in the momentum space as is in undoped LaMnO_3 , but the scattering intensities in the low energy excitations of $x = 0.2$ are anisotropic as well as temperature dependent, which indicates a reminiscence of the orbital nature.

PACS numbers: 78.70.Ck, 71.27.+a, 71.20.-b, 75.47.Gk

I. INTRODUCTION

Strongly correlated electron systems (SCES), in particular the transition metal oxides, have attracted much attention for more than a decade. They provide not only many novel physical properties, such as high temperature superconductivity, enhanced anomalies in the conductivity, etc. but the playground for the elucidation of the most fundamental subject of many-body interactions of electrons as well as the interplay of different freedoms of charge, spin, orbital and lattice. Manganese perovskites often called as manganites now become extremely important materials for this reason, in particular of the colossal magneto-resistance (CMR) effect. The CMR effect has been primarily discussed as the result of mutual interactions of various freedoms and then important issues are much relied on the search of the electronic structure in the manganites. More precisely, the effect of the strong electron correlations and the interactions with spin and orbitals determine the momentum dependence of the electron energies near the Fermi energy which is modified from the typical Fermi liquid picture in the textbook. Such electronic structure can be thoroughly explored by the detailed experiments of searching the charge dynamics in various manganites. In this respect, the resonant inelastic x-ray scattering (RIXS) is an ideal tool for the elucidation of the electron excitations, since it gives direct notion of momentum dependent spectrum. There exist several reports of such studies since the pioneering work on NiO by Kao et al.¹. Recently the RIXS measurements have been directed to both cuprates^{2,3,4,5,6,7} and manganites⁸. For the purpose of the present research, the RIXS study in LaMnO₃ of the progenitor of the CMR compounds is briefly summarized here⁸. Three salient peaks appear at the transferred energies of 2.5, 8 and 11 eV by injecting photons of the resonant energy corresponding to the Mn *K* absorption edge. The lowest excitation peak appeared at 2.5 eV was assigned to be the excitations from the occupied effective lower Hubbard band (LHB) which consists of hybridized O *2p* and Mn *3d* orbitals to the empty upper Hubbard band (UHB) based on the theoretical calculation of the RIXS process⁹. The excited electron changes the character of orbital from $3d_{3x^2-r^2}/3d_{3y^2-r^2}$ to $3d_{y^2-z^2}/3d_{z^2-x^2}$. Experimental facts of a weak momentum dependence and the apparent polarization dependence of the scattering intensity are consistent with the theoretical calculations. Two other resonant peaks at higher transition energies were also assigned to be charge transferred excitations from the inner O *2p* band to the partially filled Mn *3d* band and the empty band of hybridized *4s/4p* orbital, respectively.

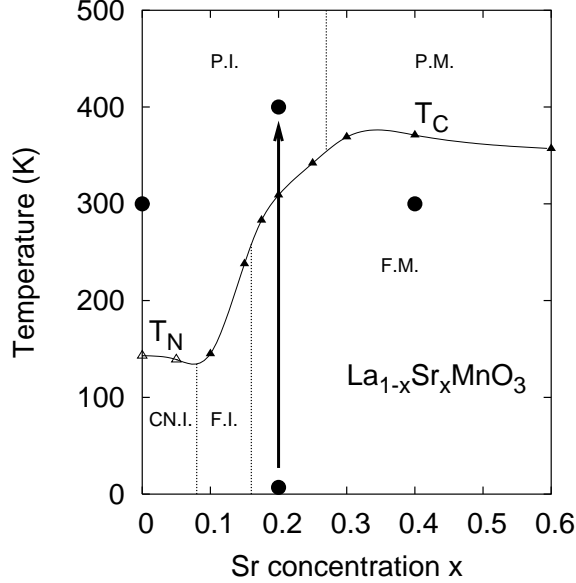


FIG. 1: Electronic phase diagram of $\text{La}_{1-x}\text{Sr}_x\text{MnO}_3$ for the Sr concentration (x) and temperature (T) from a reference¹⁰. The filled circles and the arrow indicate the observed points in Fig. 3 and 6, respectively.

Our primary goal of the present RIXS studies is to observe the excitation spectra from the metallic phase of the transition metal oxides, because novel properties appear in the vicinity of the metal insulator transition (MIT) by the carrier doping into the Mott insulators. No publications on the RIXS studies in the metallic phases exist so far, though we hear numerous experimental efforts to elucidate the nature in the metallic state. We report here the experimental results of the RIXS measurements from the doped $\text{La}_{1-x}\text{Sr}_x\text{MnO}_3$ which is compared with the previous result of the undoped LaMnO_3 ($x = 0$). The effect of the carrier doping on the low energy excitations is focused by taking two representative crystals ($x = 0.2$ and 0.4) and two different phases of either insulator or metal as shown in Fig. 1 of a simplified phase diagram of $\text{La}_{1-x}\text{Sr}_x\text{MnO}_3$. In particular, the temperature dependent features were elucidated in $x = 0.2$ crystal, where the phase transition from metal to insulator occurs associated with the ferromagnetic transition governed by the double exchange mechanism. The recent studies also suggest melting of the orbital long range order at this MIT. Therefore it is worth to search the effect of the orbital to the electronic excitations across the MIT boundary.

II. EXPERIMENTAL

We carried out the RIXS experiments at the beam line 11XU at SPring-8. A spectrometer for inelastic x-ray scattering was installed in this beam line¹¹. Incident x-rays from a SPring-8 standard undulator were monochromatized by a diamond (111) double crystal monochromator, and were focused on a sample by a horizontal mirror. A Si (333) channel cut secondary monochromator was inserted before the horizontal mirror when high energy resolution is required. Horizontally scattered x-rays are analyzed in energy by a diced and spherically bent Ge (531) crystal. The polarization vector of incident x-rays and the scattering vector are in the horizontal plane. The energy resolution in the experiments was 230 meV estimated from the full width half maximum (FWHM) of quasielastic scattering, when the Si (333) monochromator was used. The energy resolution without the Si(333) monochromator is about 500 meV. Single crystals of $\text{La}_{0.6}\text{Sr}_{0.4}\text{MnO}_3$ and $\text{La}_{0.8}\text{Sr}_{0.2}\text{MnO}_3$ were used.

The improvement of the energy resolution using the Si(333) monochromator is crucially important in this study. We could observe the peak feature of the excitation from the LHB to the UHB in high resolution experiment (Fig. 3(a)), while we could not see it in the low energy resolution (Fig. 2).

First we measured the spectra varying the energy of incident x-ray (E_i) at the fixed scattering vector $\mathbf{Q} = (2.7, 0, 0)$ to determine a resonant energy. Though the crystal structure of $\text{La}_{0.6}\text{Sr}_{0.4}\text{MnO}_3$ is rhombohedral¹⁰, we use the index of $Pbnm$ orthorhombic notation to compare easily with our previous paper⁸. All the data of this compound were taken at room temperature. The results are shown in Fig. 2. Three resonantly enhanced features can be seen at the shoulder of the elastic peak, 8 eV, and 12 eV near the K absorption edge of Mn. The resonant energy is slightly different in each excitation. The scattering intensity of the excitation at the shoulder of the elastic peak becomes strong at $E_i = 6.556$ keV, while those of 8 eV and 12 eV reach their maxima at higher E_i . The difference of resonant energy between the excitations was also observed in LaMnO_3 ⁸ and La_2CuO_4 ⁷, which indicates that the intermediate state involved in the excitation is different. Hereafter the energy of incident x-ray was selected at 6.556 keV to focus mainly on the excitation at low energy.

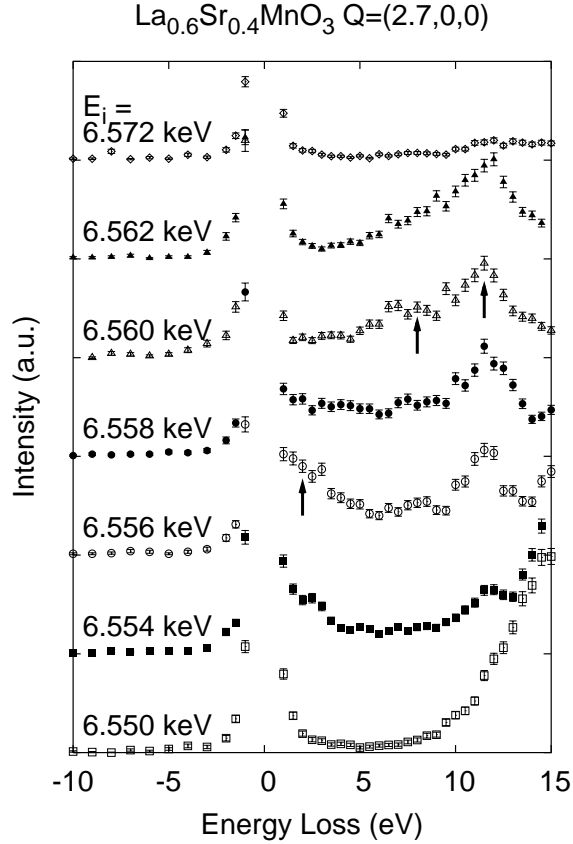


FIG. 2: Resonant inelastic x-ray scattering spectra of $\text{La}_{0.6}\text{Sr}_{0.4}\text{MnO}_3$ as a function energy loss at some representative incident x-ray energies (E_i). The energy resolution is about 500 meV, and the scattering vector is fixed at $Q = (2.7, 0, 0)$. Three resonantly enhanced excitations are indicated by the arrows. The strong intensity above 10 eV in the spectrum of $E_i = 6.550$ keV comes from the Mn $K\beta_5$ emission line.

III. RESULTS AND DISCUSSION

A. Doping dependence of RIXS spectra

RIXS spectra of $\text{La}_{1-x}\text{Sr}_x\text{MnO}_3$ are shown in Fig. 3(a), where each x and T corresponds to the filled circle in Fig. 1. Upper two curves in the figure were taken in the insulating phase, and lowers are those in the metallic phase. It should be emphasized first that a salient peak commonly appears at around 2 eV besides peaks at higher energies of 8 and 12 eV. The peak in the lowest energy can be assigned to be the electron excitations from the LHB to the UHB as mentioned in the introduction. Looking closely at the spectra, the spectral weight

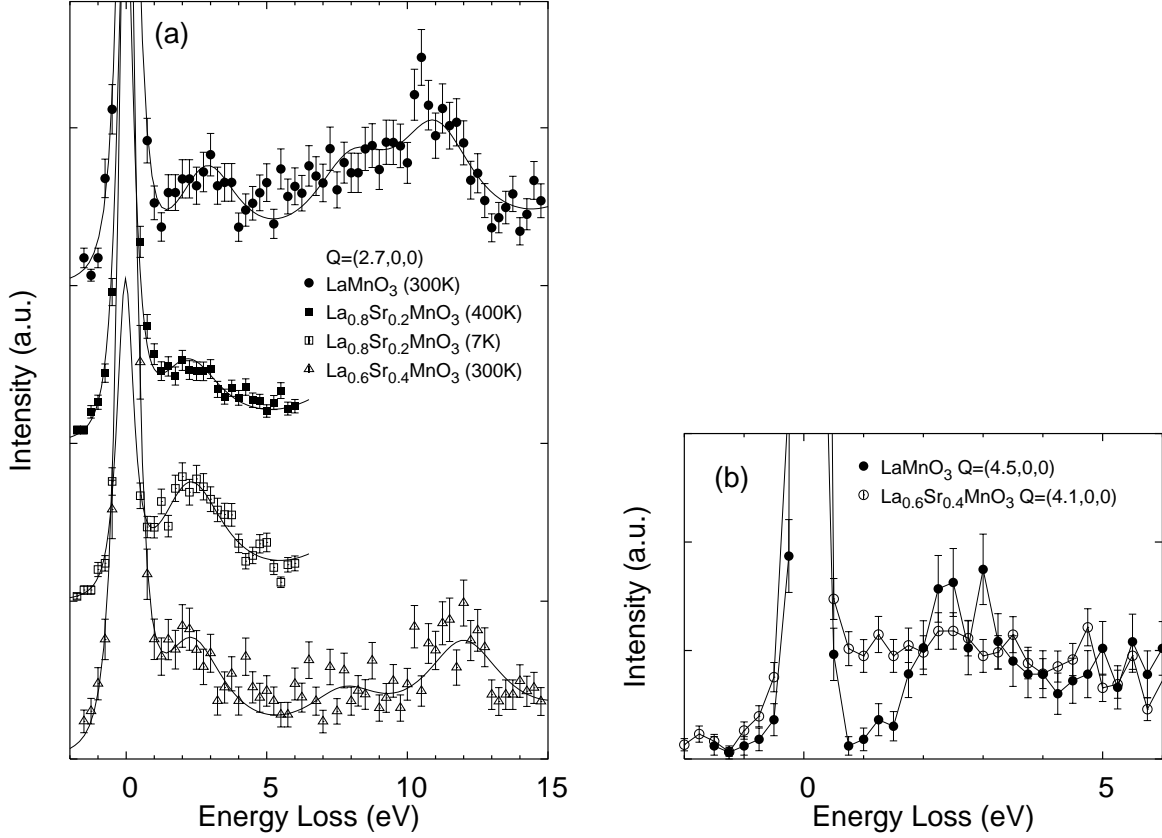


FIG. 3: Resonant inelastic x-ray scattering spectra of $\text{La}_{1-x}\text{Sr}_x\text{MnO}_3$ ($x = 0, 0.2, 0.4$). The energy resolution is about 230 meV. (a) RIXS spectra at $Q = (2.7, 0, 0)$. The solid lines are fitting results assuming the elastic peak, three Lorentz functions for excitations, and fluorescence ($\text{Mn-K}\beta_5$ line). (b) The excitation in the low-energy region measured at high scattering angle.

of these peaks tends to shift toward lower energy by the hole-doping. The experimental fact of the decrease of the energy gap between two separated e_g bands suggests the decrease of electron correlations by the hole doping, which overcomes lower shift of Fermi energy in the LHB.

Another important difference between two excitation spectra of LaMnO_3 and $\text{La}_{0.6}\text{Sr}_{0.4}\text{MnO}_3$ is more clear in the data taken at higher scattering angle (2θ) of almost 90 degree. A set of the high resolution spectra of LaMnO_3 and $\text{La}_{0.6}\text{Sr}_{0.4}\text{MnO}_3$ are depicted in Fig. 3(b). The intensity of incoherent elastic scattering is nearly proportional to $\cos^2 2\theta$ in our experimental conditions, namely, the π -polarization of incident x-ray is used, and the elastic scattering is weak at $2\theta \sim 90$ degree. Since the momentum dependence of the energy

dispersion for the lowest excitations is quite small, the difference of momentum between two spectra in Fig. 3(b) is not important. A gap feature was clearly observed in the spectrum of LaMnO_3 , while the gap is partially filled in $\text{La}_{0.6}\text{Sr}_{0.4}\text{MnO}_3$.

Even though the Hubbard gap is filled in $\text{La}_{0.6}\text{Sr}_{0.4}\text{MnO}_3$, fairly large spectral weight remains at the excitation from the LHB to the UHB, and forms the peak feature, as seen in Fig. 3(a). It gives the direct evidence of the strongly correlated electron nature.

It is natural that the origin of the excitations at 8 and 12 eV in $\text{La}_{0.6}\text{Sr}_{0.4}\text{MnO}_3$ is similar to that in LaMnO_3 . The excitations at 8 and 11 eV in LaMnO_3 are the charge transfer (CT) excitations from the O $2p$ orbitals to the Mn $3d$ and Mn $4s/4p$ orbitals, respectively. In $\text{La}_{0.6}\text{Sr}_{0.4}\text{MnO}_3$ the former corresponds to the excitation at 8 eV, and the latter is that at 12 eV. The peak position of the excitation from O $2p$ to the Mn $4s/4p$ is different between LaMnO_3 (11 eV) and $\text{La}_{0.6}\text{Sr}_{0.4}\text{MnO}_3$ (12 eV), as seen in Fig. 3(a). Probably it comes from different valence state of the manganese atom. LaMnO_3 has only one valence state of manganese atom (Mn^{3+}), while $\text{La}_{0.6}\text{Sr}_{0.4}\text{MnO}_3$ has two (Mn^{3+} and Mn^{4+}). Interatomic distance between Mn^{4+} and surrounding oxygen is shorter than that between Mn^{3+} -O. The shrinkage of the bond length makes the hybridization between O $2p$ and Mn $4p$ orbitals strong. The energy level of the Mn $4p$ orbital becomes higher because it forms mainly an anti-bonding orbital, while the energy level of O $2p$ bonding orbital becomes lower. As a result, the excitation energy increases in the highly oxidized manganese.

B. Momentum and azimuthal angle dependence of $\text{La}_{0.6}\text{Sr}_{0.4}\text{MnO}_3$

The RIXS spectra of $\text{La}_{0.6}\text{Sr}_{0.4}\text{MnO}_3$ at various scattering vectors are presented in Fig. 4(a) where solid lines show the result of the fitted curves. In orthorhombic notation of $\text{La}_{0.6}\text{Sr}_{0.4}\text{MnO}_3$, $h = 4$ and $h = 3$ correspond to the Brillouin zone center and the zone boundary, respectively. The momentum transfer dependence in the spectral shape was found to be small. In order to elucidate the dispersion relation quantitatively, we analyzed the observed data by fitting to the Lorentzian with the fixed energy width of the excitations at 3 eV. The tail of the elastic scattering or quasi-elastic component in the energy loss side (Stokes) was evaluated from the energy gain side (anti-Stokes). The observed intensities near 6 eV were considered to contain a tail from the peak at 8 eV in part, and therefore the contribution from the peak at 8 eV was taken into. The calculated spectral shape was fitted

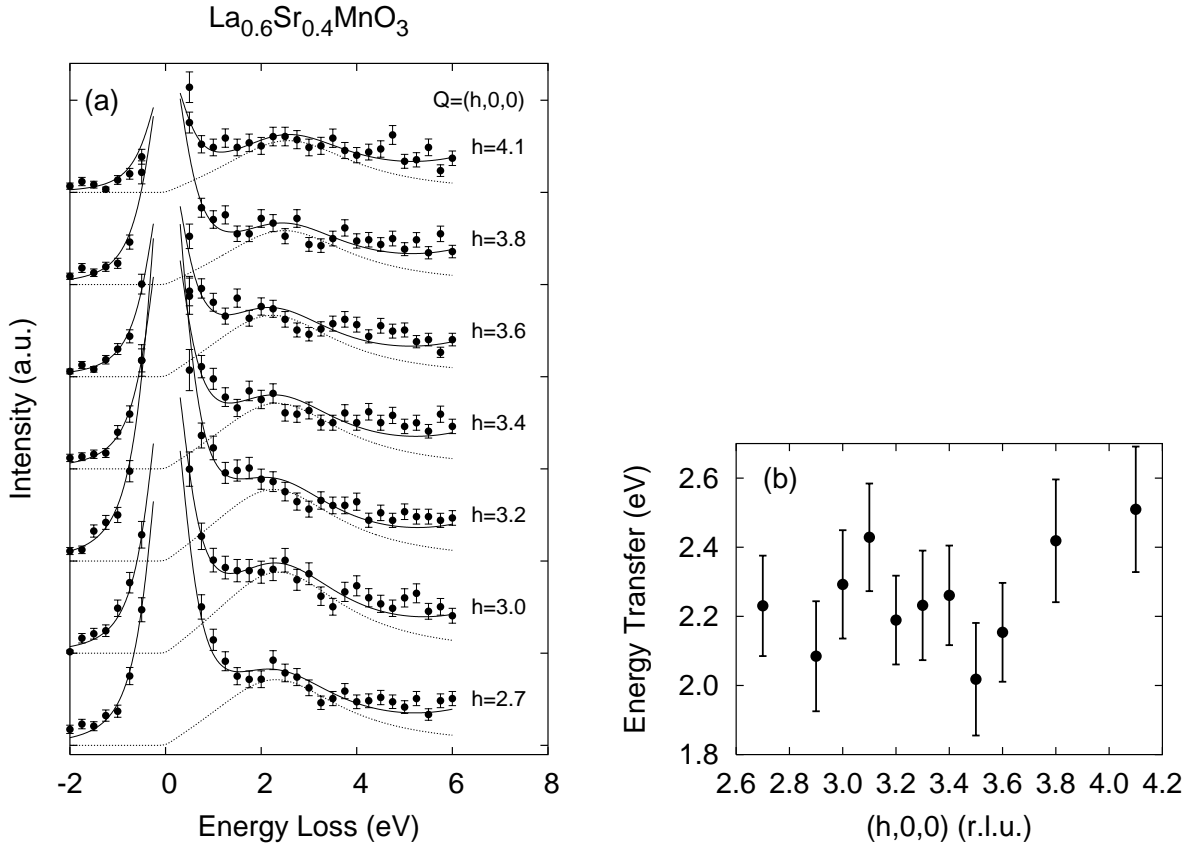


FIG. 4: (a) : The RIXS spectra of $\text{La}_{0.6}\text{Sr}_{0.4}\text{MnO}_3$ at various scattering vectors. The energy resolution is about 230 meV. Solid circles are observed points. Solid and dashed lines are the results of fitting of overall spectra and excitations from LHB to UHB, respectively. (b) : Dispersion relation of the excitation from the LHB to the UHB.

well as seen in the figure. The obtained peak positions corresponding to the gap energy between the LHB and the UHB are plotted in Fig. 4(b). The magnitude of the dispersion is small and at most 0.4-0.5 eV in total, which is comparable to that of LaMnO_3 .

In general, the RIXS spectra are approximated as the convolution of the occupied band and unoccupied band. In LaMnO_3 where the orbital long-range order is realized, the occupied LHB band consists of the orbital state represented by either $3d_{3x^2-r^2}$ or $3d_{3y^2-r^2}$ wave function which is alternately aligned. Thence the unoccupied state should be $3d_{y^2-z^2}/3d_{z^2-x^2}$. As a result, hopping to the nearest neighbor site in the UHB is forbidden in the ab plane because of the orthogonality of the wave functions. This is the reason why the UHB of LaMnO_3 is narrow and the band dispersion is flat. This fact also gives a weak dispersion relation in RIXS in LaMnO_3 . On the other hand, due to the fact of no

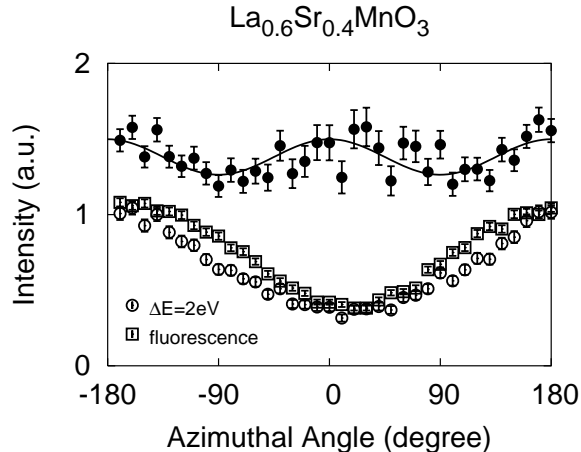


FIG. 5: Azimuthal angle (ψ) dependence of $\text{La}_{0.6}\text{Sr}_{0.4}\text{MnO}_3$. The open circles and squares are the scattering intensity of the energy transfer 2 eV at $\mathbf{Q} = (2.7, 0, 0)$ and the fluorescence yield, respectively. The filled circles represent the scattering intensity divided by the fluorescence. The solid lines are the fitting result using a function of $A(1 + B \cos^2 \psi)$.

orbital long range order in $\text{La}_{0.6}\text{Sr}_{0.4}\text{MnO}_3$, hopping to the nearest neighbor can be allowed in the UHB which gives rise to the larger dispersion relation. The observed dispersion of the excitation spectrum of $\text{La}_{0.6}\text{Sr}_{0.4}\text{MnO}_3$, however, is comparable to that of LaMnO_3 . This result can be possibly understood when the ferromagnetic metal of $\text{La}_{1-x}\text{Sr}_x\text{MnO}_3$ has a short range correlation of orbitals where the fluctuation of the orbital is enough slow compared to the transition time of the x-rays. Slow fluctuation of the orbital is regarded as a static disorder for the x-rays, and also the excited electrons seem to be far from the band electrons. Incoherent carrier motion in the crystal can be considered as a kind of localization, and the weak dispersion observed in $\text{La}_{0.6}\text{Sr}_{0.4}\text{MnO}_3$ is naturally comprehensible.

This scenario of the short range orbital correlation was also supported by another experiment of the polarization dependence of the scattering intensity. We presented the azimuthal angle dependence of the scattering intensity of 2 eV and the fluorescence as the reference in Fig. 5. Both show the oscillation of 2π period, which probably comes from the difference between the angles of incidence and reflection. When we divide the scattering intensity of 2 eV by the fluorescence yield, we can clearly see the two-fold symmetry, which is reminiscent of the case of LaMnO_3 . In the LaMnO_3 , the two-fold symmetry in the azimuthal angle dependence is stronger and the characteristics of the orbital excitation from the orbital ordered

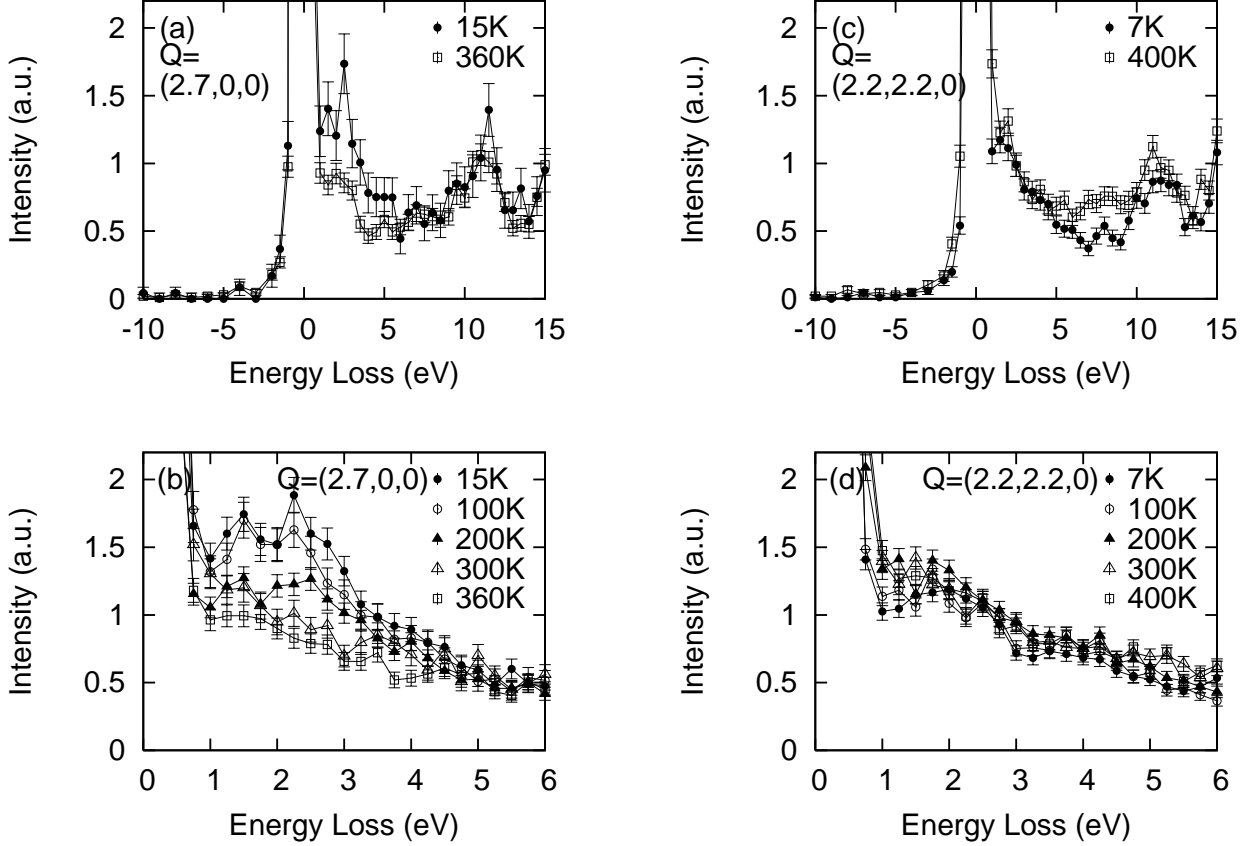


FIG. 6: RIXS spectra of $\text{La}_{0.8}\text{Sr}_{0.2}\text{MnO}_3$ at some temperatures. The energy resolution is about 500 meV. The scattering vectors are $\mathbf{Q} = (2.7, 0, 0)$ for (a) and (b), and $\mathbf{Q} = (2.2, 2.2, 0)$ for (c) and (d).

phase. We evaluated the ratio of the oscillating part to the constant part using a function of $A(1 + B \cos^2 \psi)$, where ψ is the azimuthal angle. The origin of the ψ is defined when c^* lies in the scattering plane. We obtained $B = 0.38$ and 0.19 for LaMnO_3 and $\text{La}_{0.6}\text{Sr}_{0.4}\text{MnO}_3$, respectively. The smaller value of B for $\text{La}_{0.6}\text{Sr}_{0.4}\text{MnO}_3$ may be attributed to the shorter correlation length.

C. Temperature dependence of $\text{La}_{0.8}\text{Sr}_{0.2}\text{MnO}_3$

In this section we focus on the result of $\text{La}_{0.8}\text{Sr}_{0.2}\text{MnO}_3$ which shows the MIT at 309 K, associated with the ferromagnetic phase transition¹⁰. It also shows a structural phase transition at 100 K from rhombohedral to orthorhombic¹². We measured the RIXS spectra

across two transition temperatures, as indicated by the arrow in Fig. 1.

The RIXS spectra of $\text{La}_{0.8}\text{Sr}_{0.2}\text{MnO}_3$ measured at several representative temperatures are shown in Figs. 6. The spectra are similar to those of $\text{La}_{0.6}\text{Sr}_{0.4}\text{MnO}_3$ in Fig. 2; there are three excitations at 2 eV, 8 eV, and 11.5 eV. The scattering intensity at 2-4 eV increases with decreasing temperature at $\mathbf{Q} = (2.7, 0, 0)$ (Figs. 6(a) and (b)). In contrast, the intensity of $\mathbf{Q} = (2.2, 2.2, 0)$ is nearly independent of temperature (Figs. 6(c) and (d)). It should be noted that the excitations at 11.5 eV is independent of temperature in both scattering vectors. The spectra of $\mathbf{Q} = (3.3, 0, 0)$ were confirmed to show similar temperature dependence to those of $\mathbf{Q} = (2.7, 0, 0)$, and the spectra of $\mathbf{Q} = (2.6, 2.6, 0)$ is independent of temperature. We emphasize here the experimental fact that the temperature dependence in intensity depends on the direction of scattering vector: in other words, the temperature dependence of the inter-band excitations from the LHB to the UHB is quite anisotropic.

The temperature dependence of RIXS intensity can be compared with that of the optical conductivity. The spectral weight of the optical conductivity in $\text{La}_{0.8}\text{Sr}_{0.2}\text{MnO}_3$ shifts gradually from 1-2 eV to lower energy (< 1 eV) with decreasing temperature¹³. The strength of the optical conductivity at around 2 eV decreases with decreasing temperature. Surprisingly, the temperature dependence of the RIXS intensities of $\mathbf{Q} = (2.7, 0, 0)$ is opposite to that of the optical conductivity ($\mathbf{Q} = \mathbf{0}$), namely, the intensities along $\langle h00 \rangle$ direction increase with decreasing temperature. Furthermore, the RIXS intensities show no obvious temperature dependence along $\langle hh0 \rangle$. Since the RIXS can measure the excitation at the finite momentum transfer, the electronic excitations of $\text{La}_{0.8}\text{Sr}_{0.2}\text{MnO}_3$ should be correctly understood by taking account of momentum dependence. The qualitatively different temperature dependence just suggests the influence of the orbital to the electronic conductivity, which has often been discussed.

A key to understand the temperature dependence as well as the anisotropy of RIXS intensity is the transfer of electrons near the Fermi energy. The double exchange interaction plays an essential role for the stabilization of the ferromagnetic long range order in this hole doped $\text{La}_{1-x}\text{Sr}_x\text{MnO}_3$ compounds. Because the probability of the spin-flip excitations in the RIXS process is much smaller than that of the spin-non-flip excitations, the ferromagnetic spin order of e_g electrons increases the transition probability from the LHB to the UHB. In this sense, the change in RIXS intensity along $\langle h00 \rangle$ may be attributed to the evolution of double exchange ferromagnetic interaction. The temperature dependence of scattering

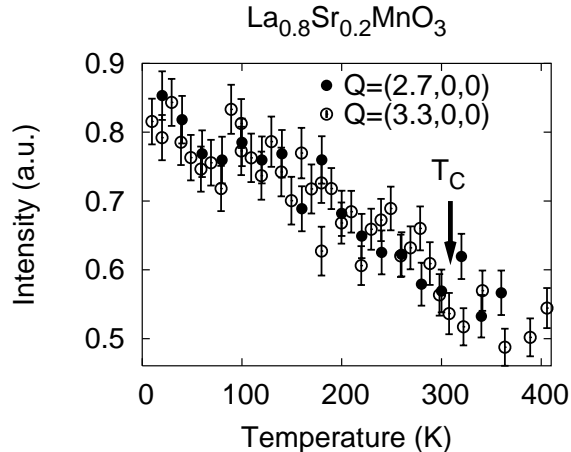


FIG. 7: Temperature dependence of the RIXS intensity at fixed energy transfer of 2.25 eV in $\text{La}_{0.8}\text{Sr}_{0.2}\text{MnO}_3$. The arrow indicates the ferromagnetic transition temperature (T_C).

intensity of 2.25 eV at $\mathbf{Q} = (2.7, 0, 0)$ and $(3.3, 0, 0)$ in Fig. 7, which qualitatively accords to that of the bulk magnetization¹⁰: the intensity begins to increase at T_C , and saturates around 150 K. On the other hand, the scattering intensity is independent of temperature along $\langle hh0 \rangle$ (Mn-O-Mn direction), which might be reflected from the ferromagnetic super-exchange interaction which is active in both metallic and insulator phases.

The present results demonstrate that the temperature dependence of the electronic excitation is quite anisotropic in $\text{La}_{0.8}\text{Sr}_{0.2}\text{MnO}_3$, and the RIXS is a powerful technique to study electronic excitation, especially in an anisotropic system, because it can provide a plenty information of the electronic excitation with *finite* momentum transfer.

IV. CONCLUSION

In conclusion, we have measured resonant inelastic x-ray scattering spectra of hole-doped manganese oxides, $\text{La}_{0.8}\text{Sr}_{0.2}\text{MnO}_3$ and $\text{La}_{0.6}\text{Sr}_{0.4}\text{MnO}_3$, and studied electronic excitations across the Mott-Hubbard gap near the Fermi energy.

The salient peak structure which corresponds to the excitation from the LHB to the UHB was observed in both $\text{La}_{0.8}\text{Sr}_{0.2}\text{MnO}_3$ and $\text{La}_{0.6}\text{Sr}_{0.4}\text{MnO}_3$, and the peak position shifts to lower energy than that of LaMnO_3 . Furthermore, the spectral weight extended to lower energies than the Mott-Hubbard gap in metallic $\text{La}_{0.6}\text{Sr}_{0.4}\text{MnO}_3$, though the peak of inter-band excitation like LaMnO_3 still maintains. This is the first RIXS experiments in which

some characteristics of the strong electron correlation are elucidated in the metallic state. The excitations from the LHB to the UHB in $\text{La}_{0.6}\text{Sr}_{0.4}\text{MnO}_3$ shows weak dependence on the momentum transfer, and the magnitude of the dispersion is 0.4-0.5 eV. The scattering intensity contains a component of the two-fold symmetry in the azimuthal angle dependence, though no static orbital order appears. All these characteristics of the inter-band excitations from the LHB to the UHB indicate that the local correlation effect is strong even in $\text{La}_{0.6}\text{Sr}_{0.4}\text{MnO}_3$.

In $\text{La}_{0.8}\text{Sr}_{0.2}\text{MnO}_3$, we found a clear temperature dependence in intensity around 2-4 eV. The RIXS intensity of $\mathbf{Q} = (2.7, 0, 0)$ increases with decreasing temperature, while the scattering intensity of $\mathbf{Q} = (2.2, 2.2, 0)$ is independent on temperature. It is a remarkable contrast with the optical conductivity, whose spectral weight at 2 eV decreases with decreasing temperature. The anisotropic temperature dependence might be attributed to an anisotropy of the ferromagnetic exchange interaction. Even though the energy dispersion is small in $\text{La}_{1-x}\text{Sr}_x\text{MnO}_3$, we could demonstrate a momentum dependent feature of the electronic excitations by the RIXS technique for the first time in the sense that the temperature dependence of the scattering intensity is anisotropic. Furthermore, the importance and usefulness of the RIXS measurements are recognized throughout the present studies because the momentum dependent electronic excitations in the manganite systems reveal the mutual interactions between charge, spin and orbital.

Acknowledgments

We acknowledge to Dr. P. Abbamonte for making the Ge analyzer. This work was supported financially in part by Core Research for Evolutional Science and Technology (CREST), sponsored by the Agency of the Japan Science and Technology.

* Electronic address: kenji@spring8.or.jp

¹ C.-C. Kao, W. A. L. Caliebe, J. B. Hastings, and J.-M. Gillet, Phys. Rev. B **54**, 16361 (1996).

² J. P. Hill, C.-C. Kao, W. A. L. Caliebe, M. Matsubara, A. Kotani, J. L. Peng, and R. L. Greene, Phys. Rev. Lett. **80**, 4967 (1998).

- ³ P. Abbamonte, C. A. Burns, E. D. Isaacs, P. M. Platzman, L. L. Miller, S. W. Cheong, and M. V. Klein, *Phys. Rev. Lett.* **83**, 860 (1999).
- ⁴ K. Hämäläinen, J. P. Hill, S. Huotari, C.-C. Kao, L. E. Berman, A. Kotani, T. Idé, J. L. Peng, and R. L. Greene, *Phys. Rev. B* **61**, 1836 (2000).
- ⁵ M. Z. Hasan, E. D. Isaacs, Z.-X. Shen, L. L. Miller, K. Tsutsui, T. Tohyama, and S. Maekawa, *Science* **288**, 1811 (2000).
- ⁶ M. Z. Hasan, P. A. Montano, E. D. Isaacs, Z.-X. Shen, H. Eisaki, S. K. Sinha, Z. Islam, N. Motoyama, and S. Uchida, *Phys. Rev. Lett.* **88**, 177403 (2002).
- ⁷ Y. J. Kim, J. P. Hill, C. A. Burns, S. Wakimoto, R. J. Birgeneau, D. Casa, T. Gog, and C. T. Venkataraman, *Phys. Rev. Lett.* **89**, 177003 (2002).
- ⁸ T. Inami, T. Fukuda, J. Mizuki, S. Ishihara, H. Kondo, H. Nakao, T. Matsumura, K. Hirota, Y. Murakami, S. Maekawa, et al., *Phys. Rev. B* **67**, 045108 (2003).
- ⁹ H. Kondo, S. Ishihara, and S. Maekawa, *Phys. Rev. B* **64**, 014414 (2001).
- ¹⁰ A. Urushibara, Y. Moritomo, T. Arima, A. Asamitsu, G. Kido, and Y. Tokura, *Phys. Rev. B* **51**, 14103 (1995).
- ¹¹ T. Inami, T. Fukuda, J. Mizuki, H. Nakao, T. Matsumura, Y. Murakami, K. Hirota, and Y. Endoh, *Nucl. Inst. & Mech. in Phys. Res. A* **467-468**, 1081 (2001).
- ¹² H. Kawano, R. Kajimoto, M. Kubota, and H. Yoshizawa, *Phys. Rev. B* **53**, R14709 (1996).
- ¹³ E. Saitoh, A. Asamitsu, Y. Okimoto, and Y. Tokura, *J. Phys. Soc. Jpn.* **69**, 3614 (2000).